

Optimized Semi-implicit Methods for Modeling Cardiac Propagation

Riasat Khan¹ and Kwong T. Ng²

¹Department of Electrical and Computer Engineering
North South University, Dhaka, Bangladesh
riasat.khan@northsouth.edu

²Department of Electrical and Computer Engineering
New Mexico State University, Las Cruces, NM 88003, USA
ngnsr@nmsu.edu

Abstract — Computer simulation of cardiac electrophysiology is now considered a powerful tool for exploring the causes of cardiac arrhythmias. Cardiac electric propagation has been studied using the monodomain model to describe wave propagation of action potential in the heart. The governing nonlinear reaction-diffusion partial differential equation is solved with the semi-implicit (implicit-explicit) method that does not have the stability limit of the explicit time-stepping scheme. Both first order and second order semi-implicit techniques for temporal discretization are considered in this paper. Second order finite difference technique is used to discretize the spatial derivatives. An explicit finite difference scheme with 512×512 nodes and $0.1 \mu\text{s}$ time step is used as the benchmark for error calculation. APPSPACK, a parallel pattern search optimization software, is used to obtain the optimal semi-implicit parameters that give the lowest root-mean-square error. Results are presented for the semi-implicit techniques with or without the operator split or protective zone method. They demonstrate that the optimized second order semi-implicit method gives the best overall performance.

Index Term — Derivative-free optimization method, monodomain model, operator split method, pattern search algorithm, semi-implicit scheme.

I. INTRODUCTION

The complex bidomain model is arguably the most comprehensive mathematical model for simulating electrical activities in the heart [1]. According to this model, the cardiac tissue is considered as two overlapping continuous domains, representing the interstitial and intracellular regions illustrated in Fig. 1. An electric potential, known as the transmembrane potential or action potential, is produced between these two domains when an electrical stimulus is applied. With the propagation of this action potential across the cardiac tissue, an electric

field is generated at the surface of the human body, giving rise to the electrogram. The bidomain model consists of coupled nonlinear reaction-diffusion and elliptical equations. Disregarding the interstitial region transforms the bidomain model into a simplified monodomain model, also known as the reaction-diffusion or cable model, which involves a single nonlinear reaction-diffusion equation [2]. The simplification of the bidomain model leads to a significantly less intensive computational solution, and recently Potse et al. showed that the discrepancy in simulated action potential propagation between the two models is negligible [3]. This confirms the use of the monodomain model as a preliminary step to develop new numerical techniques.

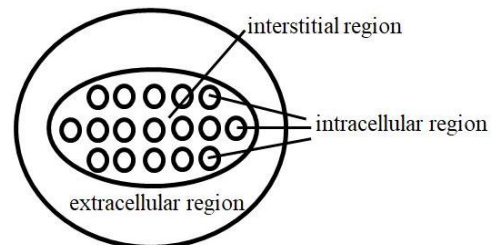


Fig. 1. Illustration of the intracellular, interstitial, and extracellular region.

The cardiac monodomain equation consists of a temporal derivative, a spatial Laplacian, and nonlinear ionic current terms. The central finite difference technique with second-order accuracy has been used to approximate the Laplacian. The ionic current introduces nonlinearity and is represented as a complex nonlinear function of the action potential. The temporal derivative has been commonly discretized with the explicit method [1], though it has a stability constraint that seriously limits the time step size. In this work, temporal discretization is achieved with the semi-implicit or implicit-explicit scheme, in which the implicit method is used for the

spatial Laplacian but the explicit method is employed for the ionic current. This mixed approach eliminates the stability limit of the explicit method, while avoiding the expensive solution of a nonlinear matrix equation required in a fully implicit method. Both first and second order semi-implicit techniques with one and two discretization coefficients, respectively, have been implemented.

A major objective of this study is to find the above coefficients that give the best results, i.e., the lowest root-mean-square (RMS) error potential. The pattern search algorithm has been applied to find these optimal parameters by using the asynchronous parallel pattern search package, APPSPACK. APPSPACK uses derivative-free optimization to minimize the objective function by changing the design variables [4]. To our knowledge, this is the first time a second order technique or parameter optimization is considered in semi-implicit finite difference modeling of cardiac propagation.

II. CARDIAC MONODOMAIN MODEL

The monodomain model is a mathematical model that describes the flow of electrical current in the heart. The governing monodomain equation is given by:

$$\frac{\partial V_m}{\partial t} = \frac{1}{C_m} \left\{ \frac{1}{\beta} [\nabla \cdot (\bar{\sigma}_i \nabla V_m) + I_{si}] - \Sigma I_{ion} \right\}, \quad (1)$$

where V_m is the action potential, i.e., the difference between the intracellular and interstitial potentials, C_m is the cell membrane capacitance per unit area, β is the membrane area per unit volume, and $\bar{\sigma}_i$ denotes the intracellular conductivity tensor. I_{si} is the intracellular source current that initiates the activation, and ΣI_{ion} represents the total ionic current through the membrane.

In this study, the ionic current ΣI_{ion} is obtained as the sum of six different types of ionic currents using the Luo-Rudy model [5]. The Luo-Rudy model is a comprehensive ionic current model that is capable of reproducing electrocardiograms similar to those recorded from patients.

III. SEMI-IMPLICIT MONODOMAIN FORMULATION

Both the first and second order semi-implicit methods have been derived from the formulation proposed by Ascher et al. [6] for partial differential equations. The update equation for the first order semi-implicit temporal discretization is given by:

$$\underbrace{\left[I - \frac{\theta \Delta t}{C_m \beta} [D_o] \right]}_{[A]} \underbrace{\bar{V}_m^{n+1}}_{\bar{x}} = \underbrace{\bar{V}_m^n + \frac{(1-\theta)\Delta t}{C_m \beta} [D_o] \bar{V}_m^n + \Delta t \left[\frac{1}{C_m \beta} I_{si}^{n+1} - \frac{1}{C_m} \Sigma I_{ion}^n \right]}_{\bar{b}}, \quad (2)$$

where $[I]$ is the identity matrix, $0 \leq \theta \leq 1$ is the discretization coefficient, Δt is the time step size, n is

the time step index, the bar designates a vector containing all the nodal values of the corresponding quantity, and $[D_o] \bar{V}_m$ represents the finite difference approximation of the Laplacian. Equation (2) represents a matrix equation, which is solved with the Jacobi preconditioned conjugate gradient iterative technique.

The second order semi-implicit discretization of the monodomain equation can be derived as:

$$\underbrace{\left\{ \left(\theta + \frac{1}{2} \right) [I] - \frac{\Delta t \left(\theta + \frac{c}{2} \right)}{C_m \beta} [D_o] \right\}}_{[A]} \underbrace{\bar{V}_m^{n+1}}_{\bar{x}} = 2\theta \bar{V}_m^n - \left(\theta - \frac{1}{2} \right) \bar{V}_m^{n-1} + \frac{\Delta t}{C_m \beta} \left[(1 - \theta - c) [D_o] \bar{V}_m^n + \frac{c}{2} [D_o] \bar{V}_m^{n-1} \right] + \frac{\Delta t}{C_m} \left[\frac{[(1 + \theta) \Sigma I_{ion}^n - \theta \Sigma I_{ion}^{n-1}]}{\bar{b}} \right] + \frac{\Delta t}{C_m \beta} \bar{I}_{si}^{n+1}. \quad (3)$$

where θ and c are second order semi-implicit temporal discretization coefficients.

A. Pattern search algorithm

The pattern search algorithm [4] is used to implement the optimization of the temporal coefficients in (2) and (3). The algorithm is based on the univariate or cyclic coordinate descent method, which uses the design variables, θ and c in the present case, as coordinate directions [7]. The search direction is computed by cycling through the n design variables, yielding n iterations for each direction search cycle. As the monodomain equation involves the nonlinear ionic current, the pattern search produces a zigzag pattern as it approaches the solution. To alleviate the zigzag path's effect, the pattern search algorithm has been set to use $n + 1$ iterations for each direction search cycle. This minor modification assembles a linear combination of the previous n search directions and the optimum value of the step size for that direction in the additional iteration step.

An asynchronous parallel pattern search package, APPSPACK, is used to implement the pattern search algorithm and obtain the optimum semi-implicit coefficients [8]. Developed at Sandia National Laboratories, APPSPACK minimizes an objective function with an unconstrained or bound-constrained input;

$$\min_{l \leq x \leq u} f(x) = \sqrt{\frac{\sum_{n=1}^N (V_m^{BM} - V_m^{calculated})^2}{N}}. \quad (4)$$

In the above equation, the bound of x is an n -dimensional vector, where l and u are its lower and upper bound. The objective function is obtained as the RMS difference between the simulated action potential, $V_m^{calculated}$, and the benchmark solution, V_m^{BM} . The bounded constraints of the design variables are set to be $0 \leq \theta \leq 1$ and $0 \leq c \leq 1$. The optimum solution is obtained with an asynchronous parallel set search that satisfies the bounded constraints by choosing appropriate search directions.

B. Operator split and protective zone method

In the operator split method, the update of unknown V_m is divided into multiple steps and the time derivative is considered as the sum of several components [9]. For the semi-implicit operator split method, the update of the Laplacian and ionic current terms are performed in alternate steps with different time steps sizes Δt and Δt_i , respectively. As the ionic current involves nonlinearity and relatively fast temporal variation, it is updated with smaller time steps, i.e., $\Delta t_i < \Delta t$. In the protective zone method, the ionic current in the operator split scheme is updated with smaller time steps only when the action potential has the fastest rate of change. The operator split as well as the protective zone method was found to improve computational efficiency [10].

IV. RESULTS AND DISCUSSION

The dimensions of the cardiac tissue are 0.5 cm in x (horizontal) direction, and 0.1667 cm in y (vertical) direction and the anisotropic tissue conductivities are 0.174 and 0.0193 S/m in x and y directions, respectively. A point stimulation current pulse located at the left bottom corner of the tissue and constant in time, with duration of 1 ms, is used to excite a propagating action potential. The three different grid sizes considered are 36, 72 and 144 nodes in each direction, and a period of 12 ms is simulated. The optimization iteration stops when the variation in RMS error between the calculated and benchmark solution is less than 0.001.

A. Methods without operator split or protective zone

The optimal θ and c values (θ_{opt} and c_{opt}) have been obtained for the three different grid sizes and $\Delta t = 0.05$ ms and 0.01 ms for the first and second order semi-implicit method. Note that for the first order method, $\theta = 0$ and 0.5 correspond to the explicit and Crank-Nicolson method, respectively. As shown in Table 1, for the first order method, θ_{opt} varies from approximately 0 to 1. For the second order method, c_{opt} is approximately zero for all the cases, but θ_{opt} varies from 0.0820 to 0.443. The RMS error decreases by 1.76–4.18 times when Δt is varied from 0.05 to 0.01 ms, depending on the order and grid size. As expected, the error decreases when the grid size is increased, e.g., for $\Delta t = 0.01$ ms, it decreases by a factor of 2.21 and 3.02 for the first and second order method, respectively, when the grid size is changed from 36^2 to 144^2 . Compared to the first order method, the second order method reduces the error by 14.2–35.7%. The use of optimized parameters also allows us to achieve accuracies higher than those obtained with the common numerical schemes, with little impact on the solution time. For example, with a 144^2 grid and $\Delta t = 0.01$ ms, the error for the optimized first order method is 16.4% and 19.1% lower than that for the explicit and Crank-Nicolson method, respectively.

Table 1: RMS error and optimum coefficients for first and second order method without operator split or protective zone

Grid Size, Δt	First Order	Second Order
36^2 , 0.05 ms	25.1 mV at $\theta_{opt} = 0.998$	21.6 mV at $\theta_{opt} = 0.227$ & $c_{opt} = 0.0500$
72^2 , 0.05 ms	22.2 mV at $\theta_{opt} = 1.00$	17.6 mV at $\theta_{opt} = 0.385$ & $c_{opt} = 0.00$
144^2 , 0.05 ms	21.9 mV at $\theta_{opt} = 1.00$	17.0 mV at $\theta_{opt} = 0.443$ & $c_{opt} = 0.0100$
36^2 , 0.01 ms	13.9 mV at $\theta_{opt} = 1.00$	12.3 mV at $\theta_{opt} = 0.0820$ & $c_{opt} = 0.00$
72^2 , 0.01 ms	7.32 mV at $\theta_{opt} = 0.00200$	5.43 mV at $\theta_{opt} = 0.210$ & $c_{opt} = 0.00100$
144^2 , 0.01 ms	6.31 mV at $\theta_{opt} = 0.324$	4.06 mV at $\theta_{opt} = 0.370$ & $c_{opt} = 0.00400$

B. Methods with operator split

The operator split scheme has been implemented such that Δt_i for ionic current is five times smaller than Δt for the Laplacian term. Table 2 demonstrates the RMS error and optimum θ and c values for operator split method with different grid sizes and time steps. The operator split improves the accuracy significantly, reducing the error by 5.91–11.3 times. However, the solution time also increases by a factor of 5.79–8.38. For the first order method, θ_{opt} varies from 0.00 to 0.583. For the second order method, θ_{opt} varies from 0.287 to 0.500 while c_{opt} is still nearly zero. Except for the 36^2 grid with the larger $\Delta t = 0.05$ ms, θ_{opt} and c_{opt} values are close to those for the Crank-Nicolson Adams-Bashforth method ($\theta = 0.5$, $c = 0$). When Δt is varied from 0.05 to 0.01 ms, the error reduces by a factor of 2.05–5.05. At the same time, the error reduces by an average of 6.99% when second order instead of first order method is used. It should be noted that increasing the grid size or decreasing the time step, while reducing the error, also increases the solution time correspondingly. Changing from first order to second order method, however, has a negligible effect on the solution time. Furthermore, the use of optimized coefficients can again lead to error minimization, e.g., for a 36^2 grid and $\Delta t = 0.05$ ms, the error for the optimized second order method is 20.6% lower than that for the Crank-Nicolson Adams-Bashforth technique.

C. Protective zone method

In the protective zone method, the ionic current is updated with a smaller time step if $\left| \frac{\partial V_m}{\partial t} \right| > 0$. While this only causes an insignificant increase in the error, it reduces the solution time of the operator split approach by a factor of 2.23–2.57. According to Table 3, the effects of the different parameters with protective zone method follow the same trend seen previously in results obtained without the protective zone scheme.

Table 2: RMS error and optimum coefficients for first and second order method with operator split

Grid Size, Δt	First Order	Second Order
36^2 , 0.05 ms	3.38 mV at $\theta_{opt} = 0.285$	3.41 mV at $\theta_{opt} = 0.287$ & $c_{opt} = 0.00700$
72^2 , 0.05 ms	3.28 mV at $\theta_{opt} = 0.483$	2.83 mV at $\theta_{opt} = 0.460$ & $c_{opt} = 0.0750$
144^2 , 0.05 ms	3.32 mV at $\theta_{opt} = 0.583$	2.87 mV at $\theta_{opt} = 0.461$ & $c_{opt} = 0.0600$
36^2 , 0.01 ms	1.65 mV at $\theta_{opt} = 0.00$	1.59 mV at $\theta_{opt} = 0.497$ & $c_{opt} = 0.00200$
72^2 , 0.01 ms	0.650 mV at $\theta_{opt} = 0.527$	0.604 mV at $\theta_{opt} = 0.500$ & $c_{opt} = 0.0685$
144^2 , 0.01 ms	0.693 mV at $\theta_{opt} = 0.516$	0.658 mV at $\theta_{opt} = 0.500$ & $c_{opt} = 0.0507$

Table 3: RMS error and optimum coefficients for first and second order method with protective zone

Grid Size, Δt	First Order	Second Order
36^2 , 0.05 ms	3.42 mV at $\theta_{opt} = 0.270$	3.50 mV at $\theta_{opt} = 0.530$ & $c_{opt} = 0.0730$
72^2 , 0.05 ms	3.29 mV at $\theta_{opt} = 0.527$	2.95 mV at $\theta_{opt} = 0.462$ & $c_{opt} = 0.0100$
144^2 , 0.05 ms	3.34 mV at $\theta_{opt} = 0.566$	2.87 mV at $\theta_{opt} = 0.455$ & $c_{opt} = 0.0500$
36^2 , 0.01 ms	1.63 mV at $\theta_{opt} = 0.0460$	1.69 mV at $\theta_{opt} = 0.625$ & $c_{opt} = 0.418$
72^2 , 0.01 ms	0.656 mV at $\theta_{opt} = 0.268$	0.728 mV at $\theta_{opt} = 0.510$ & $c_{opt} = 0.0370$
144^2 , 0.01 ms	0.701 mV at $\theta_{opt} = 0.445$	0.658 mV at $\theta_{opt} = 0.500$ & $c_{opt} = 0.0519$

V. CONCLUSION

Optimization of the temporal discretization coefficients for semi-implicit finite difference modeling of cardiac propagation has been implemented with a pattern search algorithm. The proposed second order semi-implicit technique provides higher computational efficiency than the first order method used in previous studies. The operator split and protective zone schemes developed for the first order method also work for the second order method, which allows an effective tradeoff between accuracy and solution time. Moreover, the optimized coefficients result in error minimization with negligible effect on the solution time. The optimized c coefficient is close to zero for all the cases, while the other optimal coefficients show varying degrees of dependence on grid size and time step. The computational cost in finding these optimized coefficients can be amortized over the repeated simulations in physiological studies that use the same coefficients. Future research may involve the extension of the current study to higher order semi-implicit schemes and three-dimensional realistic cardiac geometries.

REFERENCES

- [1] C. S. Henriquez and W. Ying, *The Bidomain Model of Cardiac Tissue: From Microscale to Macroscale*. Springer, Boston, 2001.
- [2] S. L. Cloherty, N. H. Lovell, S. Dokos, and B. G. Celler, "A 2D monodomain model of rabbit sinoatrial node," *23rd Annual International Conference of the IEEE Engineering in Medicine and Biology Society*, Istanbul, pp. 44-47, 2001.
- [3] M. Potse, B. Dube, J. Richer, A. Vinet, and R. M. Gulrajani, "A comparison of monodomain and bidomain reaction-diffusion models for action potential propagation in the human heart," *IEEE Tran. on Biomed. Eng.*, vol. 53, pp. 2425-2435, 2006.
- [4] A. R. Conn, K. Scheinberg, and L. N. Vicente, *Introduction to Derivative-Free Optimization*. SIAM, Philadelphia, 2009.
- [5] C. H. Luo and Y. Rudy, "A model of the ventricular cardiac action potential, depolarization, repolarization, and their interaction," *Circulation Research*, vol. 68, pp. 1501-1526, 1991.
- [6] U. M. Ascher, S. J. Ruuth, and B. T. R. Wetton, "Implicit-Explicit methods for time-dependent partial differential equations," *SIAM J. Numeric. Anal.*, vol. 32, pp. 797-823, 1995.
- [7] A. Onose and B. Dumitrescu, "Adaptive cyclic and randomized coordinate descent for the sparse total least squares problem," *23rd European Signal Processing Conference (EUSIPCO)*, Nice, pp. 1696-1700, 2015.
- [8] G. A. Gray and T. G. Kolda, "Algorithm 856: APPSPACK 4.0: Asynchronous parallel pattern search for derivative-free optimization," *ACM Trans. Math. Softw.*, vol. 32, pp. 485-507, 2006.
- [9] S. Krishnamoorthi, M. Sarkar, and W. S. Klug, "Numerical quadrature and operator splitting in finite element methods for cardiac electrophysiology," *International Journal for Numerical Methods in Biomedical Engineering*, vol. 29, pp. 1243-1266, 2013.
- [10] R. Khan and K. T. Ng, "Higher order finite difference modeling of cardiac propagation," *IEEE International Conference on Bioinformatics and Biomedicine (BIBM)*, Kansas City, MO, pp. 1945-1951, 2017.